INTERNATIONAL JOURNAL FOR NUMERICAL AND ANALYTICAL METHODS IN GEOMECHANICS, VOL. 3, 305-322 (1979)

STRESS AND PORE PRESSURE CHANGES IN CLAY DURING AND AFTER THE EXPANSION OF A CYLINDRICAL CAVITY

J. P. CARTER, M. F. RANDOLPH AND C. P. WROTH
Engineering Department, University of Cambridge, England

SUMMARY

The disturbance of a clay mass, due to either the installation of a driven pile or the expansion of a pressuremeter membrane, is often modelled as a cylindrical cavity expansion. In addition, it is usual (and convenient) to assume that the expansion occurs under conditions of plane strain. For this problem a method of analysis is presented which considers the soil to be a saturated two-phase material with a pore fluid which flows according to Darcy's Law. Non-linearity in material behaviour is permitted as long as the effective stress–strain law can be written in an incremental or rate form. The use of a consolidation analysis allows the changes in effective stress and pore pressure to be determined at any stage during both the cavity expansion and the subsequent period of reconsolidation. Expansions may occur at any prescribed rate, including the very fast (undrained) and the very slow (fully drained) case. The technique is illustrated by considering the expansion of a cavity in two different types of elastoplastic soil. It is shown how these solutions may be used to model the disturbance of the soil due to pile driving.

INTRODUCTION

The expansion of a long cylindrical cavity in an infinite medium is a boundary value problem in applied mechanics that is of interest to geotechnical engineers. Solutions to this problem have been obtained for a number of ideal materials and these have been used to model the installation of piles driven into clay soils (Butterfield and Banerjee,[3] Randolph and Wroth[20]) and the expansion of a cylindrical pressuremeter in both clays and sands (Gibson and Anderson,[10] Ladanyi,[14,15] Palmer,[17] Baguelin *et al.*,[1] Prévost and Höeg,[19] Hughes *et al.*,[12] Windle and Wroth[26]). In the former application the cavity is created, i.e. the expansion is assumed to occur from a zero initial cavity radius, while the latter case involves the expansion of a pre-existing cavity. In both applications the cylindrical expansion is used to model the deformation around the pile or pressuremeter at some distance away from the end effects, i.e. away from the ground surface and the tip in the case of a pile and away from the ends of the inflatable membrane in the case of a pressuremeter.

The assumptions of plane strain and axisymmetric deformation allow some simplification in the analysis of this type of problem. However, as more complex but realistic soil models are developed and used to represent the medium containing the cavity, then the more remote becomes the possibility of obtaining closed form solutions. Particular difficulty is met when a saturated two-phase soil is considered and a prediction of the behaviour both during and after expansion is of interest. In such cases a numerical technique may be the only means of obtaining a solution. In this paper a method is suggested which may be used whenever the soil can be

0363-9061/79/0403-0305$01.00

Received 30 May 1978
Revised 2 January 1979

modelled using an effective stress–strain law which can be cast in an incremental or rate form. A coupled consolidation analysis of the Biot type (Biot[4]) is employed and this is capable of dealing with any non-linearity which may arise from either material behaviour (Small *et al.*[25]) or finite deformation (Carter *et al.*[5,6]). Excess pore pressures, stresses and radial movements may be determined at any time during and after the cavity expansion.

The solution of the consolidation problem employs the finite element technique of spatial discretization (Sandhu and Wilson,[22] Christian and Boehmer,[7] Hwang *et al.*[13]) which is capable of dealing with cavity expansions beginning with a finite radius only. However, the means by which this may be adapted to model the creation of a cavity is also suggested. Two particular soil models were selected to illustrate the computation scheme. Closed form solutions to the cavity problem have already been found for one of these materials, while for the other a numerical solution for the expansion phase is presented for the first time.

OUTLINE OF THE CONSOLIDATION ANALYSIS

In a saturated two-phase soil it is convenient to be able to chart the generation and the dissipation of pore pressure both during and after cavity expansion. For this reason a consolidation analysis is desirable. If, say, an undrained or a fully drained expansion is of interest then either may be modelled using a sufficiently fast or slow loading rate, respectively. A general consolidation analysis which allows the possibility of non-linear material laws and large (but not infinite) strains has been presented earlier (Carter *et al.*[5]), and so only the essential details are given here.

The assumption that the deformation of the soil skeleton and the flow of the pore fluid occur under conditions of plane strain and axial symmetry simplifies the analysis and means that a one-dimensional formulation may be used. The location at time t of a typical soil particle (solid) is given by its radial coordinate r. It is also convenient to work with cylindrical components of effective stress and strain, i.e. $(\sigma'_r, \sigma'_\theta, \sigma'_z)^{\mathrm{T}}$ and $\boldsymbol{\varepsilon} = (\varepsilon_r, \varepsilon_\theta, \varepsilon_z)^{\mathrm{T}}$. These are principal components because of the geometrical conditions of the problem. Compressive stresses are taken as positive. The symbol u_e is used to denote excess pore pressure and u denotes the total pressure which is the sum of the ambient and excess component. In general the quantities $\boldsymbol{\sigma}'$, $\boldsymbol{\varepsilon}'$, u_e and u will be functions of both r and t.

Because of the non-linearity associated with this problem, an incremental solution procedure is required. The basic assumptions are listed below.

(1) The response of the soil skeleton to applied stress is coupled to the movement of pore fluid through the saturated soil. At any time a mathematical expression for this link can be written as

$$\boldsymbol{\sigma} = \boldsymbol{\sigma}' + u\mathbf{m} \tag{1}$$

where

$$\mathbf{m} = (1, 1, 1)^{\mathrm{T}}$$

and

$$\boldsymbol{\sigma} = (\sigma_r, \sigma_\theta, \sigma_z)^{\mathrm{T}} \text{ are total stress components.}$$

This is known as the effective stress principle.

(2) The stress–strain law for the soil skeleton material may be written as a relationship between the increments (or rates of change) of effective stress and strain, i.e.

$$\mathrm{d}\boldsymbol{\sigma}' = D\,\mathrm{d}\boldsymbol{\varepsilon} \tag{2}$$

where D is a matrix of coefficients which may depend upon the stress history and current stress state of the soil.

(3) The flow of pore fluid through the soil is governed by Darcy's law, which for this problem must be expressed in terms of the pore fluid velocity relative to the soil skeleton, i.e.

$$n(v_f - v_s) = \frac{-k}{\gamma_w}\frac{\partial u}{\partial r} \tag{3}$$

where

n is the soil porosity,
v_f is the actual outward radial velocity of the pore fluid,
v_s is the outward radial velocity of the soil skeleton,
k is the soil permeability and
γ_w is the unit weight of pore fluid.

(4) The pore fluid, and material forming the soil skeleton are much less compressible than the two-phase soil, so that any change in volume of an element of soil is entirely due to the expulsion or absorption of water from the element. This can be written mathematically as

$$\Lambda = \frac{1}{r}\frac{\partial}{\partial r}\{rn(v_f - v_s)\} \tag{4}$$

where Λ is the rate of volume strain (compression taken as positive).

(5) At time t a typical point of the soil continuum is located in space at position r. The total stress at this position and at this time, denoted by $\boldsymbol{\sigma}(r, t)$, must be in equilibrium with all the current boundary tractions (in the absence of radial body forces). This requirement can be expressed as

$$\frac{\partial \sigma_r}{\partial r} + \frac{\sigma_r - \sigma_\theta}{r} = 0 \tag{5}$$

This equation can be expressed alternatively in terms of stress rates and together with the rate form of equation (2) governs, *exactly*, the finite deformation of the soil skeleton. For purposes of illustration consider now a time interval (t_0, t) during which the material point has moved a distance ξ from a location r_0 to its current location r. For an incremental solution, it is convenient to rewrite equation (5) as

$$\frac{\partial \Delta\sigma_r}{\partial r} + \frac{\Delta\sigma_r - \Delta\sigma_\theta}{r} = -\left\{\frac{\partial \sigma_r(r_0, t_0)}{\partial r} + \frac{\sigma_r(r_0, t_0) - \sigma_\theta(r_0, t_0)}{r}\right\} \tag{6}$$

where $\Delta\boldsymbol{\sigma} = \boldsymbol{\sigma}(r, t) - \boldsymbol{\sigma}(r_0, t_0)$ is the change in total stress experienced by the material point in the time interval (t_0, t). It is usual for non-linear problems that do not involve large deformations to assume $r \sim r_0$, so that the right-hand side of equation (6) vanishes (since equilibrium existed at the start of the increment). In such cases a numerical solution of

$$\frac{\partial \Delta\sigma_r}{\partial r} + \frac{\Delta\sigma_r - \Delta\sigma_\theta}{r} = 0 \tag{7}$$

is then sought. However, for problems in which the geometry is significantly altered during the loading process a correct solution must satisfy equation (5) or (6) and it is not sufficient to satisfy merely the approximate form, equation (7). This point is illustrated later.

The above assumptions can be incorporated into a solution of the consolidation problem by applying the Virtual Work forms of the governing finite element equations for the general problem; these are set out in Reference 5 and so are not repeated here.

SOIL SKELETON MODELS

The analysis described above can deal with any general soil model for which the effective stress–strain law can be expressed in incremental or rate form. In order to be specific only two non-linear soil models are considered in this study. Some relevant details are now given.

Model (a)

The first such model is an isotropic material which is linearly elastic until the onset of yielding. The behaviour of the elastic soil skeleton is specified by the shear modulus G and the drained Poisson's ratio ν'. Yielding is determined by the Tresca criterion, when the stresses satisfy the equation

$$\sigma_1' - \sigma_3' = 2c \tag{8}$$

where σ_1' and σ_3' are the major and minor principal effective stresses, respectively, and c is the yield strength in pure shear. Hill[11] has presented a closed form solution for the creation of a cavity in this type of material and Gibson and Anderson[10] have presented the closed form solution for the expansion of a cavity of finite initial radius. These solutions will serve as a check on the accuracy and validity of the proposed numerical calculation scheme.

Model (b)

The second ideal material is similar to a model suggested by Roscoe and Burland.[21] It is a volumetric hardening, elastoplastic material that is based on the critical state concepts (Schofield and Wroth[23]). It is capable of predicting qualitatively many of the observed features of normally consolidated and lightly overconsolidated clays and has been used in predictions of real boundary value problems with encouraging success (Wroth and Simpson,[28] Naylor,[16] Wroth,[27] Banerjee and Stipho[2]). Details of its formulation, suitable for use in finite element calculations, can be found in several sources (Zienkiewicz and Naylor,[29] Simpson,[24] Naylor,[16] Banerjee and Stipho[2]).

This material (so called 'modified Cam-clay') requires the specification of five parameters, and values for all of them may be obtained from standard laboratory tests. These parameters are:

λ, the slope of the virgin consolidation line in e–$\ln p'$ space,
κ, the mean slope of the expansion and recompression line in e–$\ln p'$ space,
e_{cs}, the value of e at unit p' on the critical state line in e–$\ln p'$ space,
M, the value of the stress ratio q/p' at the critical state condition and
G, the elastic shear modulus.

In the above definitions the symbol e refers to the current voids ratio of the soil while the quantities p' and q are given by

$$p' = \tfrac{1}{3}(\sigma_r' + \sigma_\theta' + \sigma_z') \tag{9}$$

$$q = \sqrt{[\tfrac{1}{2}\{(\sigma_r' - \sigma_\theta')^2 + (\sigma_\theta' - \sigma_z')^2 + (\sigma_z' - \sigma_r')^2\}]} \tag{10}$$

In addition to the above-listed Cam-clay parameters a full description of the material requires specification of the soil permeability k, the unit weight of the pore fluid γ_w and a knowledge of the *in situ* stresses at each point in the soil.

For stress levels within the yield surface the deformations are determined by the elastic bulk modulus K and the shear modulus G. In this model $K = (1+e)p'/\kappa$, i.e. K is stress dependent, but G is held constant, and so the model is conservative (see Zytynski *et al.*[30]). Yielding occurs whenever the stresses obey the following criterion:

$$q^2 - M^2\{p'(p'_c - p')\} = 0 \tag{11}$$

where p'_c is a hardening parameter which defines the intersection of the current ellipsoidal yield locus and the p' axis in principal effective stress space. As the material yields and hardens, plastic flow is determined by an associated flow rule. Figure 1 illustrates the essential features of the soil model.

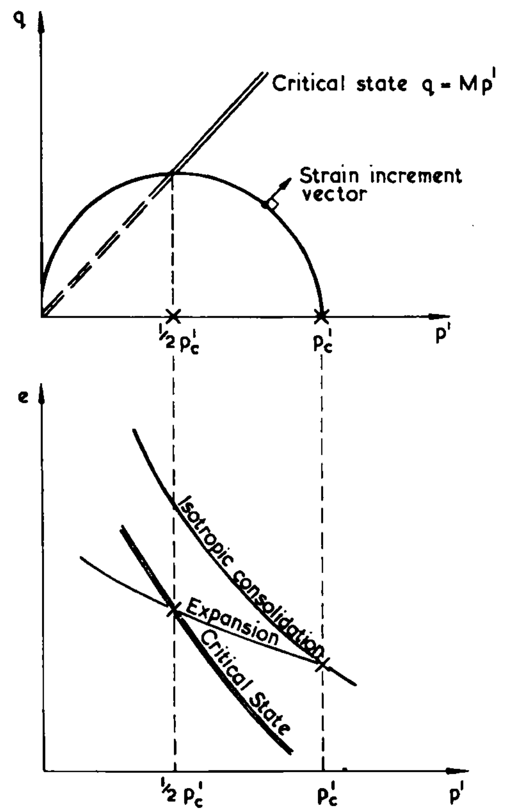

Figure 1. The work-hardening soil model

EXPANSION OF A PRE-EXISTING CYLINDRICAL CAVITY

For certain problems (e.g. the pressuremeter) prediction of the soil response is relatively straightforward because the cavity has a finite size at the start of the analysis. The numerical technique described above has been used to obtain solutions for this kind of problem and, in particular, the expansion of a long cylindrical cavity under undrained conditions in an ideal elastic, perfectly plastic material (model (a)) was considered. For convenience it was assumed that the soil surrounding the cavity was characterized by $G/c = 50$ and $\nu' = 0{\cdot}3$. Figure 2 summarizes the results of the analysis by showing the internal cavity pressure ψ plotted against the current radius a. Numerical results are plotted as individual points; these have been obtained from calculations which allowed the cavity to expand at a fast rate t approximate undrained

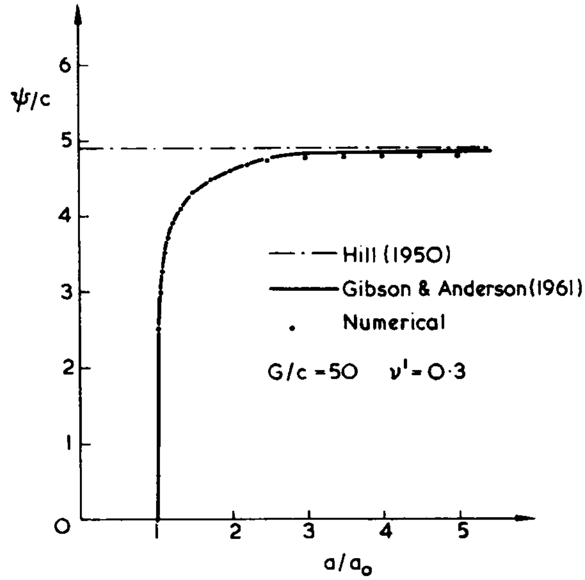

Figure 2. Solutions for the expansion of a cylindrical cavity in an elastic, perfectly plastic material

(constant volume) expansion. A closed form solution has also been found for this problem (Gibson and Anderson[10]); this is plotted as a continuous curve. The two solutions are in good agreement.

The numerical results shown in Figure 2 were obtained by ensuring that the equilibrium equation (5) was satisfied at all times. So that this could be implemented in an incremental, numerical analysis, the alternative form of equation (6) was employed, *including* the terms on the right-hand side. At the end of each increment the displacement of each finite element node was added to the current nodal coordinate before proceeding to the next step of the solution (as explained in the Appendix). Element stresses were updated in a similar manner. This procedure will be referred to as the 'total equilibrium' method.

In order to illustrate the point made earlier, Figure 3 shows a comparison of 'total equilibrium' solution with one obtained by ensuring that equation (7) was satisfied for any increment. As before, the calculated displacement increments were added to the appropriate nodal coordinates after each step. This is the same as the 'total equilibrium' method except in one important detail. The terms on the right-hand side of equation (6) have been neglected at all stages of the calculation and so equilibrium of total stress is not ensured. This latter procedure will be referred to as the 'incremental equilibrium' method.

The two numerical solutions in Figure 3 show good agreement until the cavity radius has increased to about $1{\cdot}15a_0$, i.e. $\varepsilon_\theta \sim 15$ per cent, but thereafter the 'incremental equilibrium' method overestimates the pressures which are required to cause a given expansion. In fact beyond $a \sim 1{\cdot}5a_0$ these pressures exceed the limit determined by Hill[11] and so are inadmissible. On the other hand the 'total equilibrium' solution becomes asymptotic to Hill's solution. A comparison of the distributions of total radial stress obtained using both solution techniques has been shown in Figure 4. Results are plotted for a selection of cavity sizes. At small expansions the 'incremental equilibrium' solution is in reasonable agreement with the correct solution. As the cavity enlarges the 'incremental' solution becomes more inaccurate. In contrast to this, the 'total equilibrium' solution always maintains a logarithmic variation of total radial stress with

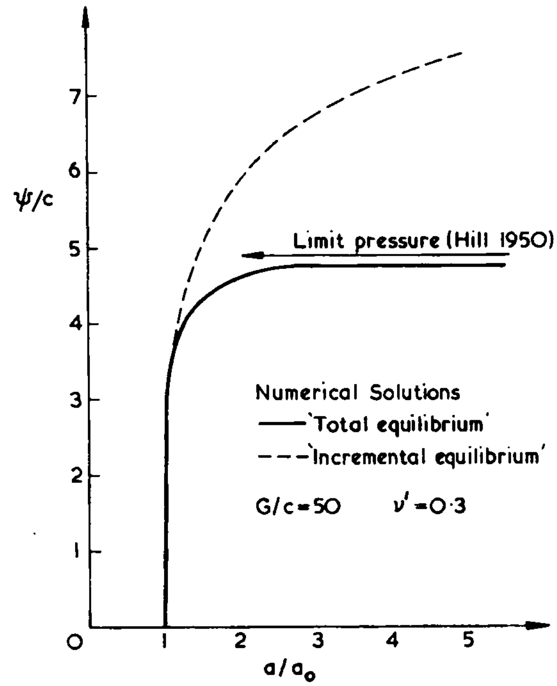

Figure 3. Comparison of 'total equilibrium' and 'incremental equilibrium' solutions

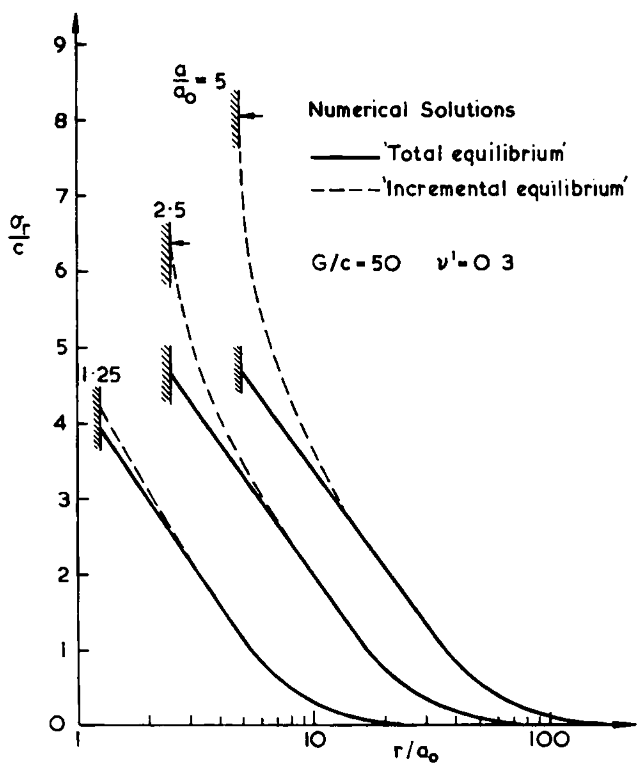

Figure 4. Stress distributions at various stages of cavity expansion

radius in the plastic region adjacent to the cavity. A logarithmic variation is necessary in order to satisfy the equilibrium equation. Once the material yields, $\sigma_r - \sigma_\theta = 2c$, and so this equation may be written as

$$\frac{d\sigma_r}{dr} + \frac{2c}{r} = 0 \tag{12}$$

Clearly care must be taken to ensure that at all times the current total stress field satisfies the equilibrium condition as expressed by equation (5). The use of equation (7) is insufficient once the deformations are large.

Further numerical details which are relevant to this type of problem can be found in the Appendix.

MODELLING THE CREATION OF A CYLINDRICAL CAVITY

In applications to such problems as the installation of a driven pile, a cavity must be created, i.e. the installation process is modelled by the expansion of a cylindrical cavity with an initial radius of zero. In contrast to this real situation, the numerical calculations must necessarily begin with a finite cavity radius to avoid the infinite circumferential strain that would occur for an initial cavity radius of zero. This restriction produces no inconsistency, however, since in plane strain the solution for expansion from a finite radius will ultimately furnish the solution to the expansion from zero initial radius. This is self evident physically; consider, for example, an outer region of the deforming soil bounded on the inside by a cylindrical surface whose radius is greater than that of the current cavity radius. In the case of undrained loading the stress and strain fields in this region are independent of conditions in the remainder; the only link with the inner material is the total radial pressure transmitted across the common interface, and it obviously makes no difference by what agency the pressure is considered to be applied. The argument is easily extended to situations in which drainage is permitted.

Consider the problem that was discussed in the previous section. For the expansion from zero initial cavity radius in a medium of ideal soil of type (a), Hill has shown that the limit pressure is reached immediately, before any displacement occurs. Hill's solution is also plotted in Figure 2 as the chain dotted curve. As noted previously the solution obtained when a pre-existing cavity is expanded asymptotically approaches Hill's solution at larger cavity radii. In fact after a doubling of cavity size the internal pressure is within 6 per cent of the ultimate limit pressure. For the expansion of a pre-existing cavity a stage is reached during the calculations after which it is unrewarding and uneconomical to continue. A suitable termination point will depend upon the choice of soil model and the selection of values for the material parameters. The authors have found that a doubling of cavity radius is adequate for both of the soil models considered in this paper. The predominant effect of expanding beyond about $a = 2a_0$ is simply to cause a further growth of the annular region of yielded soil.

Expanding a cavity from a_0 to $2a_0$ can be used to give an adequate approximation to what happens in a soil when a cavity expansion from $r = 0$ to r_0 occurs, i.e. modelling the installation into the soil of a pile of radius r_0. If both types of deformation occur at constant volume† then the necessary relation between r_0 and a_0 is

$$r_0 = \sqrt{3}a_0 \tag{13}$$

† Other volume relations may easily be adopted.

This situation is pictured schematically in Figure 5 where a vertical section is drawn through the cylinder on a diametral plane. It is evident that if such a procedure is used to model, say, a pile installation, then no knowledge is gained of the stress components and the pore pressures for the soil contained in the annular region bounded on the inside by the pile at $r = r_0$ and on the outside by the cylindrical surface at $r = 2a_0 = (2/\sqrt{3})r_0 \sim 1{\cdot}15\ r_0$. This information can only be gained from extrapolation.

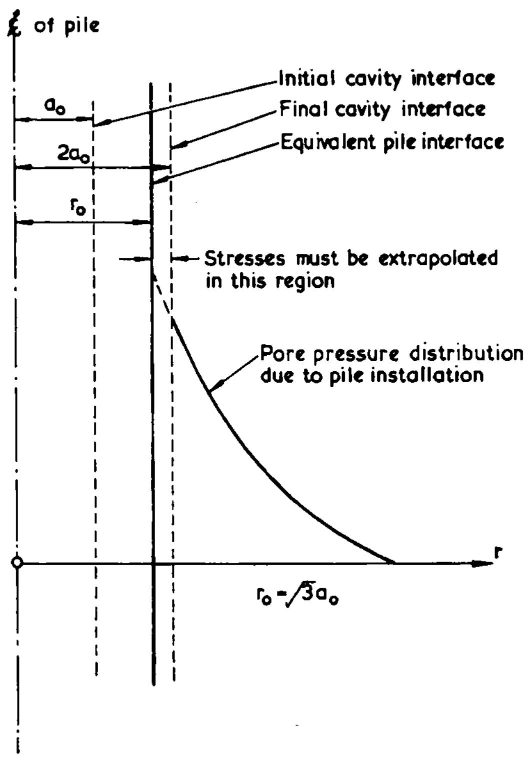

Figure 5. Finite cavity expansion as a model for pile installation

The validity and usefulness of this modelling procedure are confirmed in Figure 6 where distributions of excess pore pressure obtained using two separate computation schemes are compared. The distributions plotted as individual points were obtained from calculations which involve a doubling of the cavity radius from $a_0(\sim 0{\cdot}575r_0)$ to $2a_0(\sim 1{\cdot}15r_0)$ in a very short time interval. The cavity was then maintained at this size and excess pore pressures dissipated with drainage occurring in the positive radial direction only, i.e. the cavity interface was impermeable. At all stages of both expansion and consolidation the yielding in the soil was determined by the Tresca criterion of equation (1). The shear strength c was maintained at a constant value and was not permitted to increase with an increase in mean effective stress (as might be expected in a real soil). The distributions plotted in Figure 6 as continuous curves were calculated in the following manner. A closed form solution for the pore pressure distribution due to cavity creation (i.e. an expansion from $r = 0$ to r_0) has been suggested by Randolph and Wroth.[20] This distribution was taken as a starting point for a consolidation analysis using the numerical technique. Pore pressure dissipation was allowed to proceed assuming that the soil skeleton was

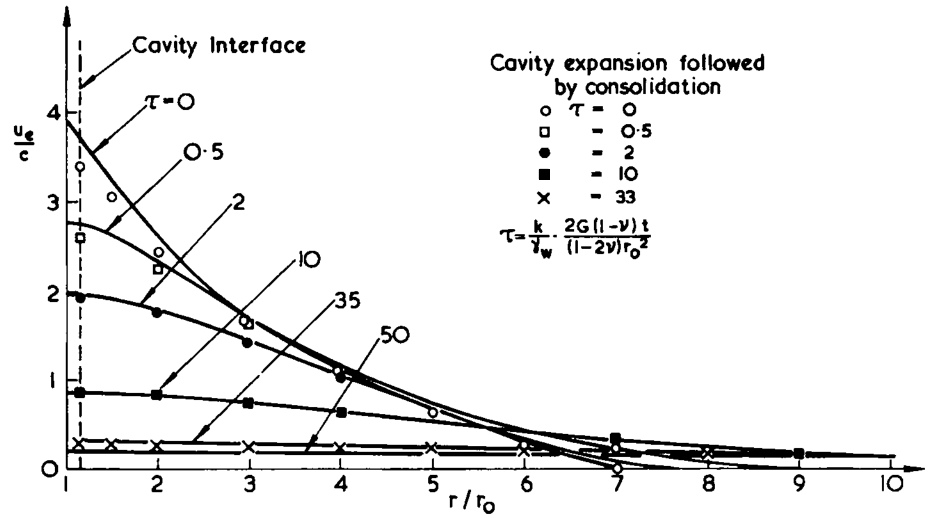

Figure 6. Comparison of pore pressure isochrones from two solution methods

again that of model (a). It can be seen from Figure 6 that the two solutions for excess pore pressure distribution agree very well for all times. The fact that a small amount of pore pressure between radii r_0 and $1{\cdot}15r_0$ has been neglected in the first instance has proved to be of little significance. In other words the consolidation which follows an undrained cavity expansion is essentially the same for the two cases of (i) cavity creation with a final radius r_0 and (ii) cavity expansion from an initial radius $0{\cdot}575r_0$ to a final radius of $1{\cdot}15r_0$.

The numerical solution for the excess pore pressure distribution immediately after doubling of the cavity is in close agreement with the expression given by Randolph and Wroth,[20] i.e.

$$\begin{aligned} u_e &= 2c \ln (R/r), \qquad && r_0 \leq r \leq R \\ &= 0, && r > R \end{aligned} \tag{14}$$

where

$$(R/r_0)^2 = G/c.$$

In addition, the radius of the plastic–elastic interface, R, is also in agreement with that quoted above. It should be pointed out that this result agrees with the solution of Hill[11] and Gibson and Anderson[10] but disagrees with the result derived by Butterfield and Banerjee.[3]

The latter result was based on a form of Von Mises failure criterion (as opposed to the Tresca criterion used here, equation (8)) and included the possibility of some shear stress on the inner wall of the cylindrical cavity. However, for the case where this shear stress is zero, the failure criterion used by Butterfield and Banerjee reduces to the Tresca criterion (see equation (1) of Butterfield and Banerjee[3]); thus the two solutions ought to provide the same expression for R/r_0.

It is perhaps worth recording here that after expansion the time dependence of the excess pore pressures is little different from that predicted for an elastic soil (Randolph and Wroth[20]). This is demonstrated in Figure 7 where the excess pore pressure at the soil cavity interface is plotted as a function of the consolidation time for both soil types. However, the same cannot be said for the stress changes that occur during consolidation. These are more dependent on the type of soil model, as can be seen from an examination of Figures 8 and 9. Figure 8 shows the total radial

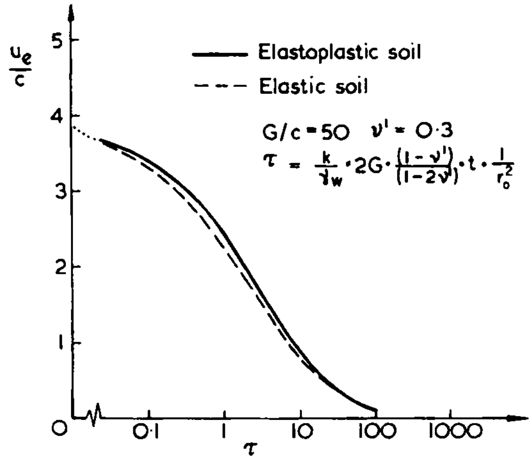

Figure 7. Decay of pore pressure with time at the cavity interface

stress σ_r and the effective radial stress σ'_r at the soil–cavity interface during consolidation while Figure 9 shows the predicted stress paths for an element of soil at the interface.

CAVITY EXPANSION AND CONSOLIDATION IN A WORK-HARDENING CLAY

For the investigation of stress and pore pressure changes due to a cavity expansion in an ideal work-hardening material (model (b)), the Cam-clay parameters were chosen to simulate a homogeneous deposit of soil like Boston Blue clay. These values were $\lambda = 0{\cdot}15$, $\kappa = 0{\cdot}03$, $e_{cs} = 1{\cdot}74$, $M = 1{\cdot}20$ and $G = 74c_u$, where c_u is the value of the undrained shear strength in plane strain. It should be noted that, since the Cam-clay yield locus is a surface of revolution about the

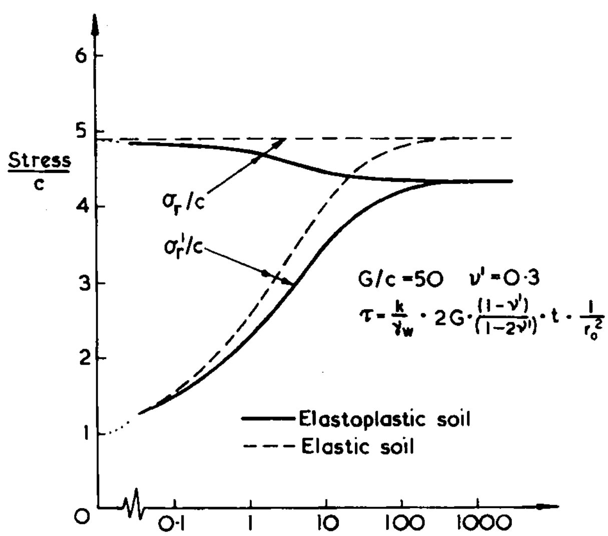

Figure 8. Changes in radial stress with time at the cavity interface

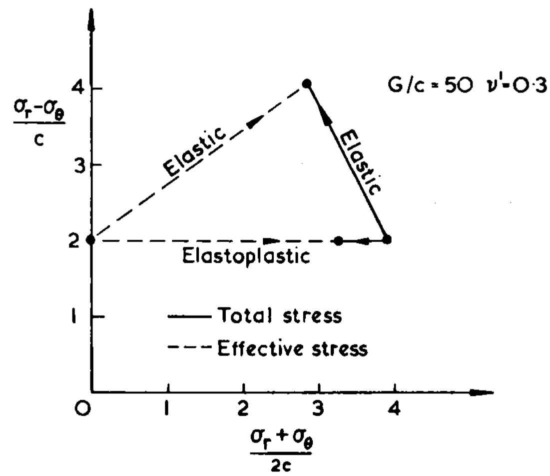

Figure 9. Stress path for soil at the cavity interface

p' axis in stress space, the value of undrained shear strength (defined as $c_u = \frac{1}{2}(\sigma_1' - \sigma_3')$) will depend on the value of the intermediate principal stress σ_2'. In a conventional triaxial test, where $\sigma_2' = \sigma_3'$, the undrained shear strength is given by $c_u = \frac{1}{2}(\sigma_1' - \sigma_3') = q_f/2$. In undrained plane strain conditions the intermediate principal stress will be equal to the average of the major and minor principal stresses and thus equation (10) yields $c_u = \frac{1}{2}(\sigma_1' - \sigma_3') = q_f/\sqrt{3}$. The plane strain value of c_u is a function of the initial voids ratio of the soil which was taken as $e = 1{\cdot}16$. The clay was also assumed to be normally consolidated with a value of $K_0 = 0{\cdot}55$, so that the *in situ* stress state was specified by $\sigma_r' = \sigma_\theta' = 1{\cdot}65c_u$, $\sigma_z' = 3c_u$ and $u_e = 0$.

Calculations were performed for the expansion of a cavity of initial radius a_0, using a fast deformation rate in an attempt to approximate an undrained expansion. The results of this analysis are presented in Figure 10 which shows the variation with cavity size (radius a) of the

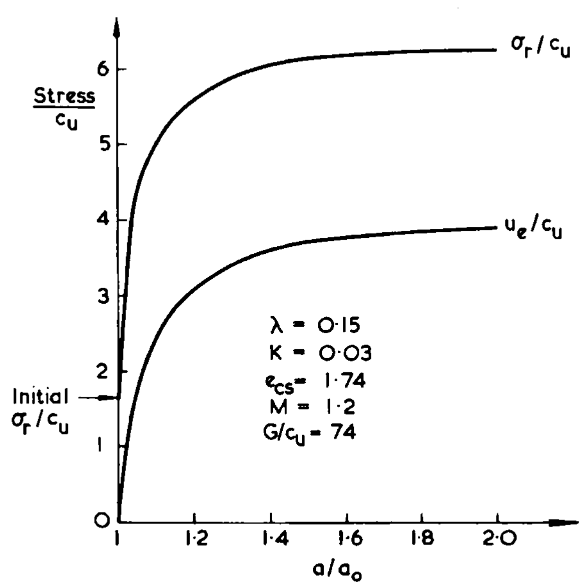

Figure 10. Pore pressure and total stress response in a work-hardening soil at the cavity interface

total internal (radial) pressure and excess pore pressure at the inner boundary. These curves show that a limit pressure is approached well before the cavity has doubled its size. The distributions of effective stress and excess pore pressure at the instant when $a = 2a_0$ are plotted in Figure 11. The process of cavity expansion has significantly altered the stress state near to the cavity interface and this effect is seen to die out with increasing radial position. Note that the

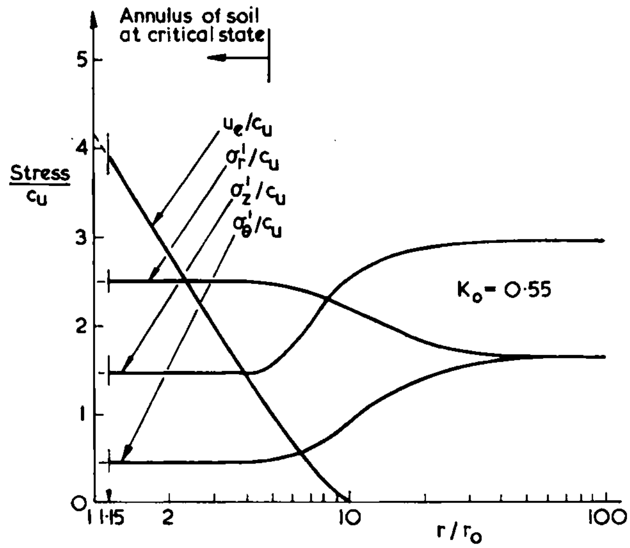

Figure 11. Stress distributions after cavity expansion in a work-hardening soil

form in which these results are presented is relevant to the case of the creation of a cavity of radius r_0 where $2a_0 = 1{\cdot}15r_0$ as before (i.e. a pile of radius r_0 installed). Also marked on this figure is the extent of the annular zone of soil in a critical state or failed condition. The remainder of the soil at larger radii is either still hardening (yielding) or remains very close to the *in situ* state. The stress condition in the region of failure is approximately uniform with a maximum stress difference of $2c_u$. It is mainly this region which exhibits the excess pore pressures.

After a doubling of the original radius the cavity size was held constant and the pore pressures dissipated with flow of pore fluid away from the impermeable inner boundary. The variation of excess pore pressure with time, measured from the completion of expansion, is shown in Figure 12(a) for soil adjacent to the cavity boundary. Figure 12(b) shows the corresponding changes in the total radial stress σ_r and the effective radial stress σ_r' during this reconsolidation period. In both plots the time t has been non-dimensionalized using a parameter τ, where $\tau = kGt/\gamma_w r_0^2$.

As the pore pressure decreases so the effective radial stress increases but, significantly, the total radial stress decreases with pore pressure dissipation. This phenomenon has been observed experimentally in the field with the Cambridge self-boring pressuremeter (Clark[8]). This is in contrast to the situation in a soil consolidating elastically where the total radial stress remains constant (Randolph and Wroth[20]).

Some idea of the stress path followed by the soil at the inner boundary can be gained from Figure 13. Here the movements in three-dimensional principal stress space are depicted by projections onto the π-plane (perpendicular to the space diagonal) and onto a plane normal to this π-plane. The p axis represents the space diagonal and τ_{oct} is the octahedral shear stress.

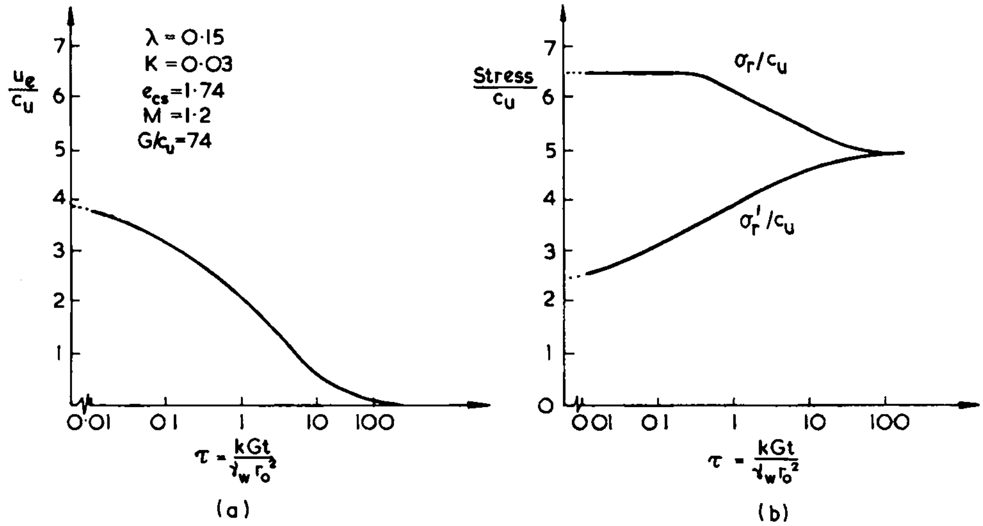

Figure 12. Variation of pore pressure and radial stress with time in a work-hardening soil at the cavity interface

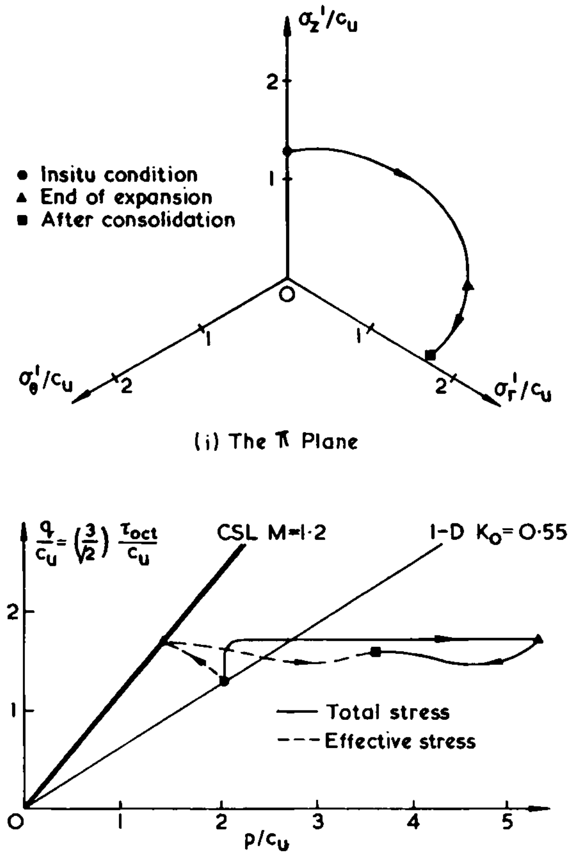

Figure 13. Stress path during cavity expansion and reconsolidation at the cavity interface in a work-hardening soil

Effective stress paths are shown by the broken curves and total stress paths by the continuous curves.

It can be seen that the soil undergoes a decrease in mean effective stress and an increase in octahedral shear stress and eventually reaches a critical effective stress state early during the expansion phase. Any further increase in total stress thereafter is borne by an equal increase in pore pressure. In contrast, the path during consolidation shows an increase in mean effective stress and a decrease in mean total stress with movement away from the critical state condition. This movement occurs at almost constant q. In the *in situ* condition the soil was in a triaxial stress state with the vertical component being the major stress. After the cavity expansion and subsequent consolidation, the stress state near the soil–cavity interface is also almost triaxial, but now the radial stress component is the major principal stress.

For an undrained cavity expansion under conditions of plane strain and axial symmetry the Cam-clay model predicts that failure is reached when $q = (\sqrt{3}/2)(\sigma_1' - \sigma_3') = \sqrt{3}c_u \sim 1{\cdot}73c_u$. The numerical results presented here are in close agreement with failure indicated at $q \sim 1{\cdot}76c_u$.

It is useful to compare the general forms of the stress changes using the work-hardening soil model, with those given by Randolph and Wroth[20] for an ideal elastic perfectly plastic soil model. In particular, during the expansion phase, the pore pressure distribution varies approximately linearly with the logarithm of the radius with a gradient of $\sim 2c_u$ (compare Figure 11 with equation (14)). During consolidation, the variation of pore pressure at the cavity edge with time is very similar irrespective of the soil model (see Figures 7 and 12). However, important differences occur in the principal stress changes during consolidation. With the work-hardening soil model (b), the deviator stress q stays almost constant during consolidation. This contrasts strongly with the solution assuming an elastic soil model (Randolph and Wroth[20]) where there is a marked increase in q.

CONCLUSIONS

A technique has been suggested that allows a determination of the stress and pore pressure changes in a saturated clay due to a cylindrical cavity expansion. Estimates of these changes can be made at any time during the expansion as well as during the subsequent period of reconsolidation. The method may be used to make predictions of the response of the surrounding soil when a pre-existing cavity is enlarged, such as in a pressuremeter test. The manner in which this technique can be extended to model the creation of a cavity is also indicated; this is relevant to the practical problem of pile installation. It is suggested that the behaviour of a shrinking cavity may also be analysed with the current method. Solutions obtained in this way may be relevant to the modelling of the soil behaviour following a tunnel excavation or borehole drilling. It is also possible to extend the present methods to perform an analysis of the expansion or contraction of a cavity under conditions of spherical symmetry.

For the cylindrical expansion problem two soil models were considered in detail. Numerical solutions showed very good agreement with closed form answers for the first of these models—an ideal elastoplastic one. A solution was then obtained for an expansion in the second, a work-hardening soil model, and the results were interpreted for the problem of pile driving. It was concluded that the dissipation of pore pressures with time is relatively unaffected by the choice of soil model and a good estimate can be obtained by assuming a linear elastic soil with a sensible choice of parameters. However, the predicted stress changes are much more dependent on the type of soil model. It is proposed to present a detailed parametric study of the effects of pile driving, using the present numerical method, in a future paper.

ACKNOWLEDGEMENTS

The work reported in this paper was supported by a research contract with Exxon Production Research Company. During the course of the research, the authors had useful discussions with Dr. T. W. Miller, Principal Engineer for Exxon, whose contribution is gratefully acknowledged.

APPENDIX

Some notes on the numerical procedure

Finite deformation of the soil skeleton is governed by equations (2) and either (5) or (6). Although written in incremental form, equation (6) is an exact expression of equilibrium, no matter what the magnitude of the radial displacement $\xi = r - r_0$. It is non-linear however, since it presumes that the location r of a soil particle at time t is known *a priori*. Any numerical solution of equation (6) will begin at some time t_0 with a knowledge of r_0 and $\boldsymbol{\sigma}(r_0, t_0)$. Some increment of time $\Delta t = t - t_0$ is specified and it is the corresponding incremental quantities ξ and $\Delta\boldsymbol{\sigma}$ which are then sought. Since finite time steps must necessarily be used in the numerical procedure a value of $r = r_0 + \xi$ has to be estimated in order that (6) may be solved. This estimation may be done iteratively but it introduces a degree of approximation‡ into the solution of (6). Note that it is the use of a numerical procedure which introduces some error into the solution, and not the use of an approximate governing equation. At the end of each step in the numerical solution the calculated increment of displacement is added to the original coordinate value, and in this way r_0 is up-dated after each step. The stresses are up-dated in a similar fashion.

The finite element mesh used to obtain the numerical results of this paper consisted of elements with three nodes, as depicted in Figure 14. Because all deformations and pore fluid movements are planar and only in the radial direction is it convenient to adopt elements where all nodes lie on the same radial line. Within each element the displacement and the excess pore pressure were taken as quadratic functions of radial position. No special numerical difficulties were met as a result of using shape functions of the same order for both pore pressure and displacement in this essentially one-dimensional problem.

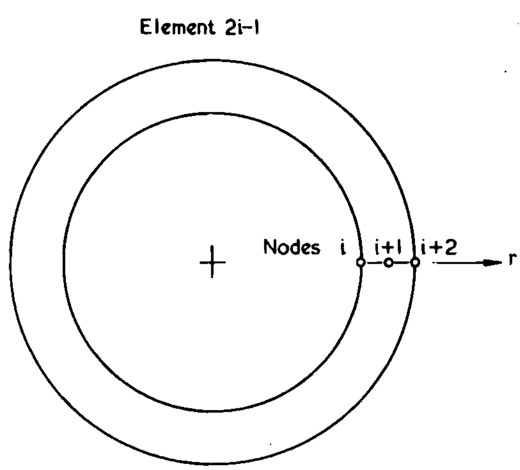

Figure 14. A typical finite element used in the one-dimensional analysis

‡ This is in addition to the approximations involved in spatial discretization using the finite element technique.

Obviously the choice of a finite element mesh to represent the continuum is limited to one of finite proportions ¶ even though in this problem the soil extends to infinity. In order to provide accurate numerical results the finite location of the outer boundary should be a sufficient distance from the cavity. It was found that this location depended on the planned magnitude of the cavity expansion. For the example of a doubling of cavity radius (from a_0 to $2a_0$) adequate results could be obtained with the boundary located at about $r \sim 50a_0$, but for an expansion from a_0 to $5a_0$ a location of $r \sim 120a_0$ was required.

In the finite element mesh employed the nodes were spaced so that the radial coordinates of any two adjacent nodes were in fixed proportion. This enabled a minimization of the error involved in numerically calculating the radial strain increment and the pore pressure gradient. Typically 200 nodes were used over a radial distance from a_0 to $50a_0$. Such a small nodal spacing is only required during the cavity expansion phase and it becomes very conservative when used to calculate the deformations that accompany the subsequent pore pressure dissipation. These consolidation movements are usually at least one or more orders of magnitude less than the movements involved in expansion.

Of course the need for close mesh spacing can be avoided, at least in some cases, if the type of analysis suggested by Palmer[17] is used. This involves following the known strain path throughout the soil, then using the stress–strain law to determine the effective stress changes and finally using the equations of equilibrium to obtain the pore pressures. This method is valid only when the strain path is known, as in an undrained cavity expansion. It is of no use if the cavity is to be expanded at a slower rate as happens, for example, in some pressuremeter tests.

Ideally for an undrained solution a time step $\Delta t = 0$ is required. However, this will involve the introduction of zeros along parts of the diagonal of the matrix of coefficients in the finite element equations. This makes many common solution procedures break down, e.g. Crout–Cholesky factorization. If such solution procedures are to be used, a close approximation to the undrained solution can be found by allowing Δt to take a very small value which is still large enough not to cause numerical problems with the inversion method. For a uniform finite element mesh (as used here) the size of this number is dictated by the requirement that

$$\Delta t > \frac{K + \frac{4}{3}G}{(k/\gamma_w)10^n}$$

where n is the number of digits used by the computer (Ghaboussi and Wilson[9]).

REFERENCES

1. F. Baguelin, J. F. Jézéquel, E. Le Mée and A. Le Méhauté, 'Expansion of cylindrical probes in cohesive soils', *Proc. ASCE*, SMFE, Divn., **98**, No. SM11, 1129–1142 (1972).
2. P. K. Banerjee and A. S. Stipho, 'Associated and non-associated constitutive relations for undrained behaviour of isotropic soft clays', *Int. J. Numer. Anal. Methods Geomech.*, **2**, 35–56 (1978).
3. R. Butterfield and P. K. Banerjee, 'The effect of pore water pressures on the ultimate bearing capacity of driven piles', *Proc. Second South East Asian Conf. on Soil Engineering*, Bangkok, 385–394 (1970).
4. M. A. Biot, 'General theory of three dimensional consolidation', *J. Appl. Phys.*, **12**, 155–164 (1941).
5. J. P. Carter, J. R. Booker and J. C. Small, 'The analysis of finite elasto-plastic consolidation', *Int. J. Numer. Anal. Methods Geomech.*, **3**, 107–129 (1979).
6. J. P. Carter, J. C. Small and J. R. Booker, 'A theory of finite elastic consolidation', *Int. J. Solids Struct.*, **13**, 467–478 (1977).
7. J. T. Christian and J. W. Boehmer, 'Plane strain consolidation by finite elements', *Proc. ASCE*, **96**, No. SM4, 1435 (1970).
8. B. G. Clarke, Private communication (1977).

¶ The infinite element concept, discussed by Pircher and Beer,[18] was not employed here.

9. J. Ghaboussi and E. L. Wilson, 'Flow of compressible fluid in porous elastic media', *UC-SESM Report No. 71-12*, Dept. of Civ. Eng., Univ. of California, Berkeley (1971).
10. R. E. Gibson and W. F. Anderson, 'Insitu measurement of soil properties with the pressuremeter', *Civ. Engng Public Works Rev.*, **56**, 615–618 (1961).
11. R. Hill, *The Mathematical Theory of Plasticity*, Oxford University Press, London 1950.
12. J. M. O. Hughes, C. P. Wroth and D. Windle, 'Pressuremeter tests in sands', *Géotechnique*, **27**, 455–477 (1977).
13. C. T. Hwang, N. R. Morgenstern and D. W. Murray, 'On solutions of plane strain consolidation problems by finite element methods', *Can. Geotech. J.*, **8**, 109–118 (1971).
14. B. Ladanyi, 'Expansion of a cavity in a saturated clay medium', *Proc. ASCE*, **89**, No. SM4, 127–161 (1963).
15. B. Ladanyi, 'In-situ determination of undrained stress–strain behaviour of sensitive clays with the pressuremeter', *Can. Geotech. J.*, **9**, 313–319 (1972).
16. D. J. Naylor, 'Non-linear finite element models for soils', *Ph.D. Thesis*, University College of Swansea, Wales (1975).
17. A. C. Palmer, 'Undrained plane-strain expansion of a cylindrical cavity in clay: A simple interpretation of the pressuremeter test', *Géotechnique*, **22**, 451–457 (1972).
18. H. Pircher and G. Beer, 'On the treatment of "infinite" boundaries in the finite element method', *Int. J. num. Meth. Engng*, **11**, 1194–1197 (1977).
19. J. H. Prévost and K. Höeg, 'Analysis of pressuremeter in strain-softening soil', *Proc. ASCE*, **101**, No. GT8, 717–732 (1975).
20. M. F. Randolph and C. P. Wroth, 'An analytical solution for the consolidation around a driven pile', *Int. J. Numer. Anal. Methods Geomech.* **3**, 217–229 (1979).
21. K. H. Roscoe and J. B. Burland, 'On the generalised behaviour of "wet" clay', *Engineering Plasticity*, Eds. J. Heyman and F. A. Leckie, Cambridge University Press, Cambridge, pp. 535–609, 1968.
22. R. S. Sandhu and E. L. Wilson, 'Finite element analysis of seepage in elastic media', *Proc. ASCE*, **95**, No. SM3, 641 (1969).
23. A. N. Schofield and C. P. Wroth, *Critical State Soil Mechanics*, McGraw-Hill, New York, 1968.
24. B. Simpson, 'Finite elements applied to problems of plane strain deformation in soils', *Ph.D. Thesis*, Cambridge University (1973).
25. J. C. Small, J. R. Booker and E. H. Davis, 'Elastoplastic consolidation of soil', *Int. J. Solids Struct.*, **12**, 431–448 (1976).
26. P. Windle and C. P. Wroth, 'The use of a self-boring pressuremeter to determine the undrained properties of clays', *Ground Engng*, Sept. (1977).
27. C. P. Wroth, 'The predicted performance of a soft clay under a trial embankment loading based on the Cam-clay model', in *Finite Elements in Geomechanics*, Ed. G. Gudehus, Chapt. 6, Wiley, London, 1977.
28. C. P. Wroth and B. Simpson, 'An induced failure at a trial embankment: Part II. Finite element computations', *Proc. Specialty Conf. Performance of Earth and Earth Supported Structures*, ASCE, Vol. 1, Pt. 1, pp. 65–80, 1972.
29. O. C. Zienkiewicz and D. J. Naylor, 'The adaptation of critical state soil mechanics theory for use in finite elements', *Proc. Roscoe Memorial Symposium*, Cambridge, Foulis, 537–547 (1971).
30. M. Zytynski, M. F. Randolph, R. Nova and C. P. Wroth, 'On modelling the unloading–reloading behaviour of soils', *Int. J. Numer. Anal. Methods Geomech.*, **2**, 87–93 (1978).